Multi-decadal ice-velocity and elevation changes of a monsoonal maritime glacier: Hailuogou glacier, China

Yong ZHANG,[1,2] Koji FUJITA,[2] Shiyin LIU,[1] Qiao LIU,[1] Xin WANG[1]

[1]*State Key Laboratory of Cryospheric Sciences, Cold and Arid Regions Environmental and Engineering Research Institute, Chinese Academy of Sciences, Lanzhou 730000, China*
E-mail: zhangy@lzb.ac.cn
[2]*Graduate School of Environmental Studies, Nagoya University, Nagoya 464-8602, Japan*

ABSTRACT. Digital elevation models (DEMs) of the ablation area of Hailuogou glacier, China, produced from Advanced Spaceborne Thermal Emission and Reflection Radiometer (ASTER) data obtained in 2009, differential GPS (DGPS) data surveyed in 2008 and aerial photographs acquired in 1966 and 1989 are differenced to estimate long- and short-term glacier surface elevation change ($\mathrm{d}h/\mathrm{d}t$). The mean $\mathrm{d}h/\mathrm{d}t$ of the ablation area over 43 years (1966–2009) is $-1.1 \pm 0.4\ \mathrm{m\ a^{-1}}$. Since 1989 the thinning has accelerated significantly. Ice velocities measured by DGPS at 28 fixed stakes implanted in the ablation area increase with distance from the glacier terminus, ranging from $41.0\ \mathrm{m\ a^{-1}}$ approaching the glacier terminus to a maximum of $205.0\ \mathrm{m\ a^{-1}}$ at the base of an icefall. Our results reveal that the overall average ice velocity in the ablation area has undergone significant temporal variability over the past several decades. Changes in glacier surface elevation in the ablation area result from the combined effects of climate change and glacier dynamics, which are driven by different factors for different regions and periods.

INTRODUCTION

Mountain glaciers cover an area of 114 800 $\mathrm{km^2}$ in central Asia (Dyurgerov, 2002), among which more than half (52% of the total) are in China (Shi and others, 2005). Glaciers in China are categorized into three types (Fig. 1) – extremely continental, sub-continental and monsoonal maritime – based on climatic conditions, especially regional annual precipitation (Shi and Liu, 2000). Glaciers are widely recognized as indicators of climate change over decades to centuries (Solomon and others, 2007). Global warming drove a strong reduction in the mass balance of most glaciers during the second half of the 20th century, resulting in remarkable retreat in China (e.g. Yao and others, 2004; Ding and others, 2006; Liu and others, 2006). In numerous studies (e.g. Lu and others, 2002; Liu and others, 2003, 2006; Shangguan and others, 2006; Ye and others, 2006; Zhang and others, 2008), only variations in glacier catchment area and extent have been considered and there has been little evaluation of glacier volumetric change or dynamic processes. In particular, far too little attention has been paid to such research on the monsoonal maritime glaciers in China.

The monsoonal maritime glaciers are located in the southeastern part of the Tibetan Plateau (Fig. 1). These glaciers cover an area of 13 200 $\mathrm{km^2}$, accounting for 22% of the total area of glaciers in China (Shi and Liu, 2000) and approximately the same area as the Southern Patagonia Icefield, the largest temperate ice mass in the Southern Hemisphere (Rignot and others, 2003). For most monsoonal maritime glaciers in China (Fig. 1), in which the summer mean air temperature is greater than –1°C and which receive abundant annual precipitation (1–3 m w.e.), the equilibrium-line altitude (ELA) is relatively low compared with other glacier types (Shi and Liu, 2000). The monsoonal maritime glaciers are the most sensitive to climate change, especially temperature change (Oerlemans and Fortuin, 1992; Fujita, 2008). Of all retreating glaciers in the world, this glacier type has exhibited the most intensive mass loss over the past few decades (Rignot and others, 2003; Kaser and others, 2006). An important feature of some monsoonal maritime glaciers in China is a supraglacial debris cover (Shi and others, 2005). The insulating effect of supraglacial debris affects how debris-covered glaciers respond to climate change (Kick, 1962; Nakawo and others, 1999; Benn and others, 2001). Ice-flow velocities on monsoonal maritime glaciers are often linked to variations in water supply to subglacial channels and conduits in which increases in water pressure result in increased basal sliding as the ice–bed interface decouples (Mair and others, 2001; Willis and others, 2003). A better understanding of the evolution and spatial variability of monsoonal maritime glaciers may contribute to better knowledge of the impact, trends and rates of ongoing climate change.

Our main purpose is to complement and extend our understanding of surface processes on monsoonal maritime glaciers by analyzing the variability in surface elevation and velocity on Hailuogou glacier, China. We first present spatial patterns of change in glacier surface elevation in the ablation area of Hailuogou glacier for the period 1966–2009, which have resulted from the combined effects of climate change and glacier dynamics. Second, we report the results of ice velocities measured at 28 stakes in the summer of 2008, and we use these and earlier studies to address the temporal variability in surface velocity.

STUDY AREA

Hailuogou glacier (29°35.6′ N, 101°56.7′ E) flows from the eastern side of Gongga mountain (7556 m a.s.l.), with a length of 13.1 km and an area of 25.7 $\mathrm{km^2}$ (Fig. 1) (Shi and others, 2005). The glacier extends from 7556 m a.s.l. to 2910 m a.s.l. at the terminus. It is representative of monsoonal maritime glaciers. The climate is dominated by the southwest and southeast monsoons in the summer and by the westerly circulation in the winter (Li and Su, 1996). The

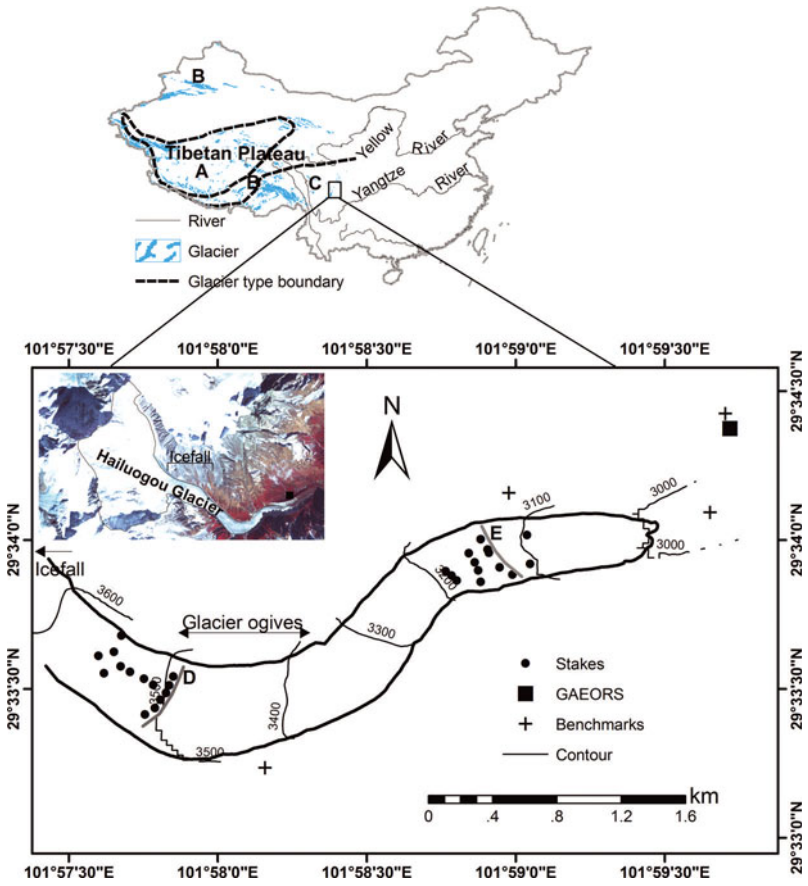

Fig. 1. Ablation area of Hailuogou glacier on the eastern side of Gongga mountain, China. The color image is a false-color ASTER image acquired on 18 January 2009 showing the catchment and glacier terminus region. The image represents a 15 km × 9 km area. Circles are the survey stakes. Crosses are benchmarks for the ground survey that are the national trigonometric reference points. The square indicates the location of Gongga Alpine Ecosystem Observation and Research Station (GAEORS) of the Chinese Ecological Research Network. A, B and C are extremely continental, sub-continental and monsoonal maritime glaciers, respectively, and their boundaries are extracted from Shi and Liu (2000). D and E are cross-sections, located at 3475 and 3110 m a.s.l., respectively.

glacier receives abundant annual precipitation (~1.9 m w.e.). In particular, the summer precipitation accounts for approximately 80% of the total annual precipitation (Su and others, 1996).

The ablation area of Hailuogou glacier is dominated by a large icefall (3650–4980 m a.s.l.; Fig. 2a) and glacier ogives (3400–3500 m a.s.l.; Fig. 2b). The icefall is characterized by rapid extending flow, which depends mainly on ice extrusion and chaotic crevassing to transport the ice downwards (Li and Su, 1996). Ogives (alternating dark and light bands on the ice surface, reflecting different thicknesses of debris covering the glacier surface) are regularly spaced and arcuate. In addition to these features, the ablation area is covered by a debris layer (Fig. 2c and d). The thickness of the debris cover increases progressively from the icefall toward the terminus, varying from 0.0 to 0.6 m according to field observations in the summer of 2008. In some locations large rocks are piled up to several metres.

DATASETS

For the analysis of ice-velocity and surface elevation change on Hailuogou glacier, we employ a variety of datasets. These include survey data using a carrier-phase differential GPS (DGPS), digital elevation models (DEMs) derived from data over different periods, surface velocity measurements, and temperature and precipitation data.

DGPS survey data

Surveys were carried out in and around the ablation area of Hailuogou glacier in June and October 2008 using carrier-phase DGPS (Magellan Promark3 and Unistrong E650). One receiver was established at a fixed base point on a rock outcrop of the glacier margin. Another was used to survey simultaneously on and around the glacier. To measure ice ablation and velocity, a 28-stake network was set up with one central longitudinal transect and six transverse transects (Fig. 1).

We surveyed an area of 0.7 km (north–south) by 3.6 km (east–west) over an altitude range of 675 m (2925–3600 m a.s.l.) in June 2008 (Fig. 3a). Data post-processing of DGPS measurements was performed using the global navigation satellite systems (GNSS) solutions (Magellan Co. Ltd). The methods used for evaluating the accuracy of DGPS data and generating a DEM based on the DGPS data of June 2008 are the same as used by Fujita and others (2008). The relative positions and altitudes of all points were calculated on the Universal Transverse Mercator (UTM) projection (zone 47N, World Geodetic System 1984 (WGS84) reference system) referenced to two peaks (Fig. 3a). Relative measurement errors in the survey are evaluated by comparing the positions of four benchmarks that were measured more than once (Fig. 1). Standard deviations of differences from the averages (12 measurements in total, three measurements for each benchmark) indicate measurement errors of 0.12 m

Fig. 2. (a) Icefall, (b) glacier ogives, (c) ablation area and (d) ice cliffs located at the terminus of Hailuogou glacier.

horizontally and 0.19 m vertically. All DGPS points surveyed in June 2008 (89 174 points) were converted into gridcells by a standard kriging method in which points utilized to obtain a gridcell altitude are limited to the circle with a radius equal to half the diagonal of the targeted gridcell. The resolution of ground-survey gridcells (hereafter called DGPS-2008) is 15 m × 15 m (Fig. 3b).

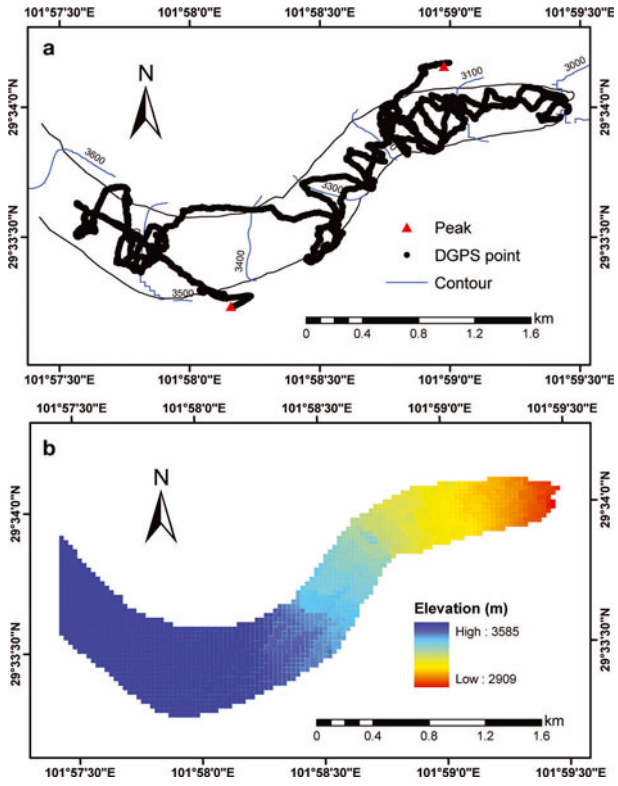

Fig. 3. (a) Distribution of DGPS points surveyed in June 2008. (b) DEM (DGPS-2008) generated by DGPS survey data in June 2008.

Digital elevation models (DEMs)

The Advanced Spaceborne Thermal Emission and Reflection Radiometer (ASTER) DEM used in the analysis is produced from data obtained from the ASTER ortho-image obtained on 18 January 2009 (Table 1; Fig. 4a), in which no cloud or snow cover was found. The spatial resolution is 15 m × 15 m. The ASTER ortho-image is generated by the ASTER Ground Data System (ASTER GDS) at the Earth Remote Sensing Data Analysis Center (ERSDAC) in Japan. The detailed algorithm for DEM generation is described by Fujisada and others (2005) or can be viewed at http://www.gds.aster.ersdac.or.jp/gds_www2002/exhibition_e/a_products_e/a_product2_e.html. The location of the ASTER visible/near-infrared (VNIR) image was affine-transformed by referring to a topographical map (see below). The root-mean-square error (RMSE) of the affine transformation was <15 m. The same transformation was adapted to the DEM.

Other DEMs were derived from the relief plate contours published by the State Bureau of Surveying and Mapping of China (SBSMC, 2000) as summarized in Table 1. These

Table 1. Elevation data sources

Source	Datum	Nominal scale	Vertical RMSE m	Acquisition year
DEM-1966	Beijing 1954	1:100 000	9.00	1966
DEM-1989	Xi'an 1980	1:50 000	11.20	1989
DGPS-2008	WGS84	–	0.19	2008
ASTER DEM	–	–	13.90	2009

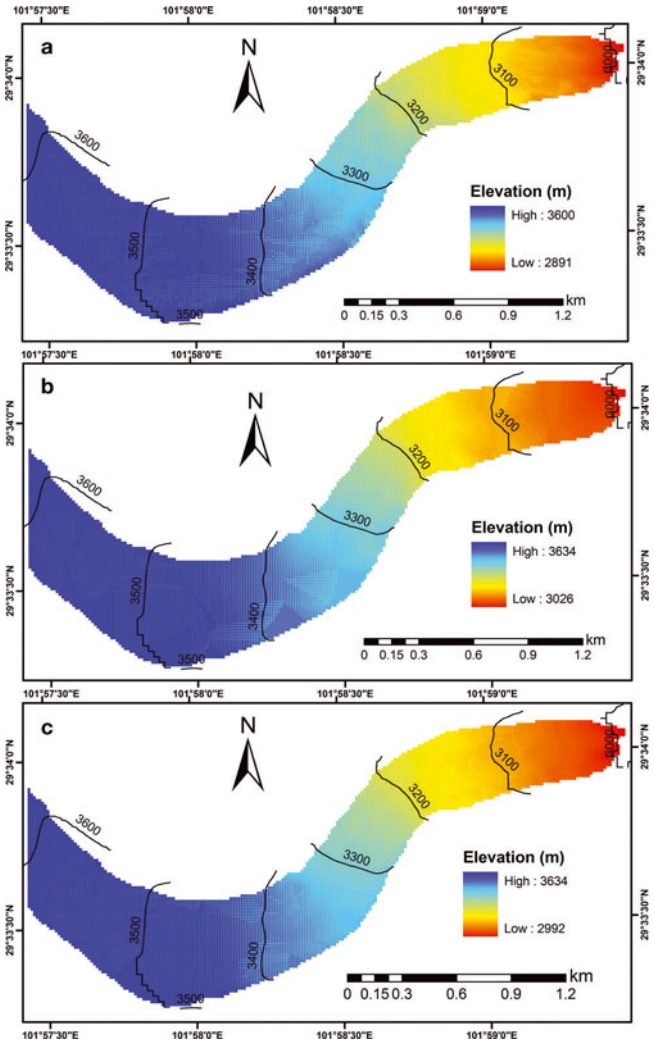

Fig. 4. ASTER DEM (a), DEM-1966 (b), and DEM-1989 (c) of the ablation area of Hailuogou glacier.

cartographies were photogrammetrically derived by SBSMC from aerial photographs acquired in 1966 and 1989 (DEM-1966 and DEM-1989) (Fig. 4b and c). The respective geodetic coordinate systems of DEM-1966 and DEM-1989 are the Beijing geodetic coordinate system 1954 and Xi'an geodetic coordinate system 1980. Nominal vertical accuracies of DEM-1966 and DEM-1989 are ~20 m and ~10 m (1/2 map contour interval), respectively (SBSMC, 2000).

In order to compare with other data, the SBSMC DEMs were re-projected onto the WGS84 UTM datum by using a seven-parameter datum transformation model based on the four known national trigonometric reference points (Fig. 1) and resampled to a 15 m × 15 m grid size for co-registration. The seven-parameter datum transformation model is given by

$$\begin{bmatrix} X_{\mathrm{WGS84}} \\ Y_{\mathrm{WGS84}} \\ Z_{\mathrm{WGS84}} \end{bmatrix} = \begin{bmatrix} \mathrm{d}X \\ \mathrm{d}Y \\ \mathrm{d}Z \end{bmatrix} + (1+k) \begin{bmatrix} 1 & \varepsilon_Z & -\varepsilon_Y \\ -\varepsilon_Z & 1 & \varepsilon_X \\ \varepsilon_Y & -\varepsilon_X & 1 \end{bmatrix} \begin{bmatrix} X_{54/80} \\ Y_{54/80} \\ Z_{54/80} \end{bmatrix}, \quad (1)$$

where X_{WGS84}, Y_{WGS84} and Z_{WGS84} are the WGS84 datum coordinates, $X_{54/80}$, $Y_{54/80}$ and $Z_{54/80}$ are the Beijing 1954 and Xi'an 1980 datum coordinates, $\mathrm{d}X$, $\mathrm{d}Y$ and $\mathrm{d}Z$ are the translation parameters, ε_X, ε_Y and ε_Z are the rotation parameters and k is the scale factor. These parameters, estimated by the four known national trigonometric reference points, are given in Table 2. Extensive discussion of the application of the seven-parameter datum transformation model to China has been provided by Guo and others (2002) and Wang and others (2003). The error using a seven-parameter datum transformation model is <0.002 m (Wang and others, 2003).

Table 2. Estimated parameters for transformations from the Beijing 1954 and Xi'an 1980 datum coordinates to the WGS84 datum coordinate based on the four known national trigonometric reference points

Parameter	Beijing 1954	Xi'an 1980	Unit
$\mathrm{d}X$	3.342242	3.342187	10^6 m
$\mathrm{d}Y$	–1.153078	–1.153059	10^6 m
$\mathrm{d}Z$	–1.8677	–1.8571	10^4 m
ε_X	–5.008	–5.008	arcsec
ε_Y	2.899	2.899	arcsec
ε_Z	–0.045	–0.045	arcsec
k	3.643	3.631	10^{-4}

Temperature and precipitation

Temperature and precipitation data for the period 1988–2004 were observed at the Gongga Alpine Ecosystem Observation and Research Station (GAEORS) of the Chinese Ecological Research Network (CERN, http://www.cern.ac.cn) (Fig. 1). GAEORS is a sub-alpine observatory located on the eastern slope of Gongga mountain at ~3000 m a.s.l. and about 1.5 km from the glacier terminus (Fig. 1). The air temperature, precipitation, humidity, wind speed and air pressure have been measured since 1988. Temperature and precipitation data used in this study were derived from the observed daily data in GAEORS. The average annual temperature and precipitation in GAEORS are 4.1°C and 1942 mm w.e., respectively, for the period 1988–2004 (Fig. 5a). The summer precipitation accounts for approximately 80% of the total annual precipitation (Fig. 5a). Annual average air temperature has experienced a significant rise, by 0.27°C $(10\,\mathrm{a})^{-1}$, over the last 17 years (1988–2004) (Fig. 5b).

Accuracies of DEMs

Fujita and others (2008) evaluated the relative accuracies of the ASTER DEM with a resolution of 15 m in the Bhutan Himalaya. The RMSE was 11.0 m in the altitudinal difference between the ASTER DEM and a DEM generated from DGPS ground-survey data (Fujita and others, 2008). Similarly, we compare the ASTER DEM with the DGPS ground-survey DEM. As shown in Figure 6a the standard deviation (i.e. the RMSE) is 13.9 m. Fujita and others (2008) pointed out that the influence of terrain slope between the gridcells is less obvious in the ASTER DEM with a resolution of 15 m, especially with the slope <40°, which accounts for 96% in our analysis. Therefore, we do not consider the influence of terrain slope within a gridcell on the altitudinal difference of the ASTER DEM.

On the other hand, the SBSMC DEMs are the dominant source of elevation errors. Vertical errors in the SBSMC DEMs were estimated relative to the DGPS survey points in a non-glacierized area. Average RMSEs of DEM-1966 and DEM-1989 are 9.0 and 11.2 m, respectively, and exhibit a normal distribution (Fig. 6b and c).

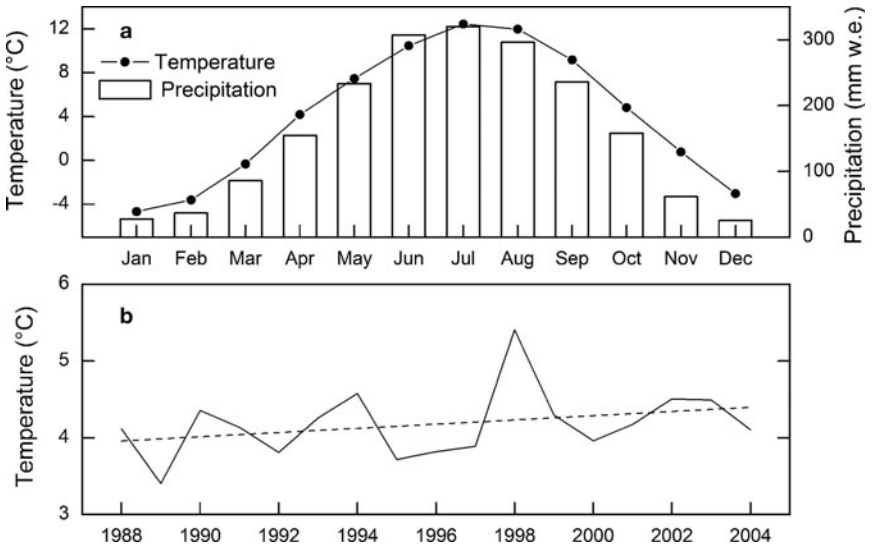

Fig. 5. Variations in (a) average monthly temperature and precipitation and (b) average annual temperature observed at GAEORS for the period 1988–2004.

RESULTS

Surface-elevation changes over 43 years

Elevation changes from 1966 to 2009 in the ablation area of Hailuogou glacier were estimated by subtracting DEM-1966 from DGPS-2008 (June 2008) and ASTER DEM (January 2009) (Fig. 7). Most of the ablation area has experienced a significant thinning over the past several decades (Fig. 7). Mean elevation change rates (dh/dt) are $-1.0 \pm 0.4\,\mathrm{m\,a^{-1}}$ for the period 1966–2008 and $-1.1 \pm 0.4\,\mathrm{m\,a^{-1}}$ for the period 1966–2009. As shown by Figure 7, the frontal tongue of the glacier has undergone a strong surface lowering over the periods considered, where the maximum dh/dt values are $-3.2 \pm 0.4\,\mathrm{m\,a^{-1}}$ for the period 1966–2008 and $-3.3 \pm 0.4\,\mathrm{m\,a^{-1}}$ for the period 1966–2009. The DGPS- and ASTER-derived dh/dt values show close agreement, suggesting any inter-technique bias is small. Conversely, about 0.5% of the ablation area for the period 1966–2008 and 1.3% for the period 1966–2009 have undergone surface rising (Fig. 7). The former mainly occurs in the zone of glacier ogives (Fig. 7a), whereas Figure 7b shows the thinning in this area. The reason is that the DGPS survey points are sparse in this area as indicated in Figure 3a.

To monitor glacier change, long-timescale (decades) observations of surface elevation are required to separate short-term fluctuations from changes that may reflect secular trends. Surface dh/dt in the ablation area was estimated for different periods: (1) 1966–89 using DEM-1989 minus DEM-1966; and (2) 1989–2009 using ASTER DEM minus DEM-1989. Estimates indicate spatially non-uniform thinning and thickening of the ablation area (Fig. 8). Mean dh/dt values for the ablation area are $-0.67 \pm 0.4\,\mathrm{m\,a^{-1}}$ during 1966–89 and $-1.61 \pm 0.6\,\mathrm{m\,a^{-1}}$ during 1989–2009. A significant common characteristic over the period considered (about 23 and 20 years, respectively) is that the terminus of Hailuogou glacier underwent dramatic thinning (Fig. 8). For the period 1966–89, the thickening mainly occurred at the base of the icefall where the mean dh/dt value is $+0.14 \pm 0.09\,\mathrm{m\,a^{-1}}$ (Fig. 7a). After 1989 most of the ablation area shows clear thinning; only about 1.3% of the ablation area experienced thickening (Figs 8b and 9).

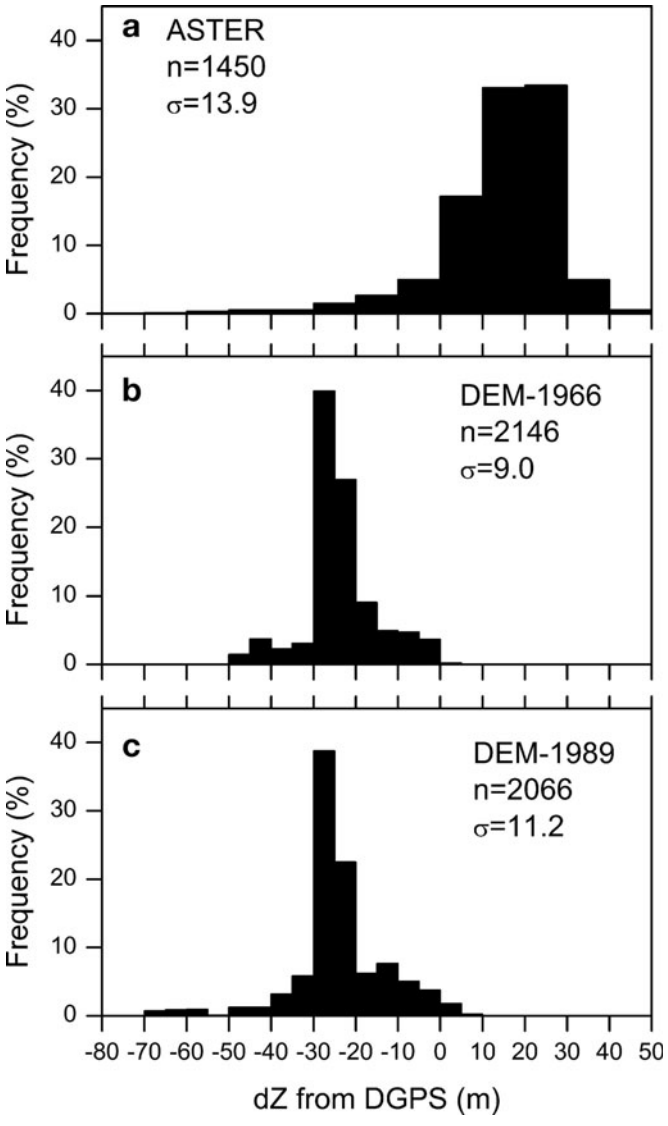

Fig. 6. Histograms of altitudinal differences at 5 m intervals of (a) ASTER DEM, (b) DEM-1966 and (c) DEM-1998.

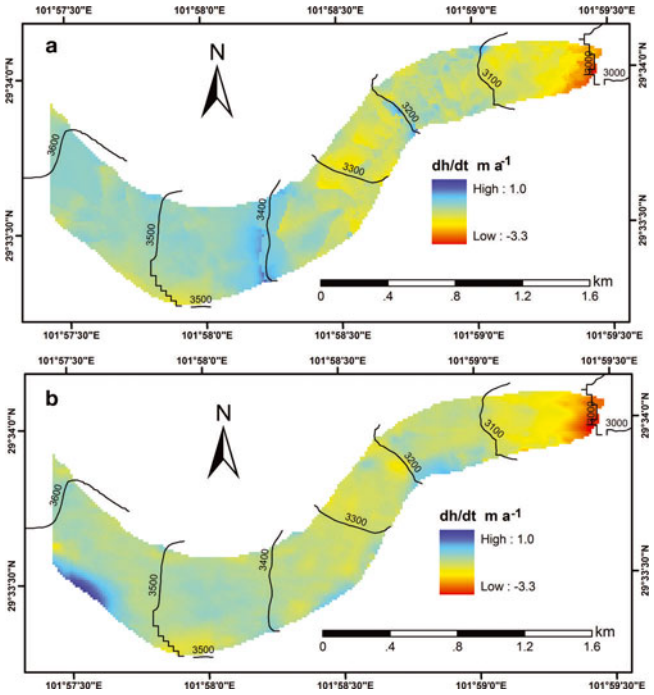

Fig. 7. Elevation change rate (d*h*/d*t*) of the ablation area. (a) 1966–2008 using DGPS-2008 minus DEM-1966 and (b) 1966–2009 using ASTER DEM minus DEM-1966.

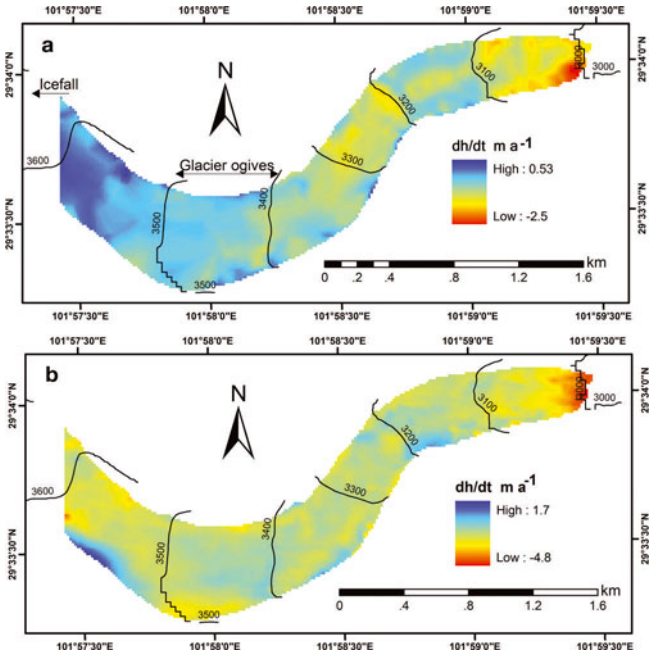

Fig. 8. Elevation change rate (d*h*/d*t*) in the ablation area. (a) 1966–89 using DEM-1989 minus DEM-1966 and (b) 1989–2009 using ASTER DEM minus DEM-1989.

In comparison with surface d*h*/d*t* for the period 1966–89, the mean thinning rate in the past 20 years has increased from 0.67 to 1.53 m a^{-1}. For the period 1966–89, about 92% of the survey area experienced surface lowering while 8% experienced surface rising (Fig. 9a). After 1989, the surface underwent a dramatic surface lowering, with about 98% of the survey area decreasing in elevation (Fig. 9c). This indicates that surface thinning in the ablation area of Hailuogou glacier has accelerated significantly since 1989. Consequently, the glacier terminus shows a very strong response, with an accelerated retreat rate. Since the 1960s the retreat of the glacier terminus has accelerated from 12.7 m a^{-1} (1966–89; Su and others, 1992) to 27.4 m a^{-1} (1998–2008).

Ice velocity and its temporal variability

Ice velocities measured in the summer of 2008 at 28 stakes in the ablation area are shown in Figure 10. In general, ice velocities in the ablation area show a clear increase with distance from the glacier terminus (Figs 10 and 11a). The velocities range from a maximum of 205.0 m a^{-1} at the base of the icefall, located at 3550 m a.s.l., to 41.0 m a^{-1} approaching the glacier terminus. A mountain glacier generally flows through a valley that may partially impede glacier flow (Nye, 1965). The effect of lateral drag on ice velocity can be seen clearly in Figure 11b. The glacier reaches its maximum velocity near the center, and the velocity decreases towards both lateral margins (Fig. 11b).

The directional consistency of the velocity vectors changes systematically along the glacier (Fig. 10). The ice-flow directions up-glacier are consistently along the zone of glacier ogives, while the measurements located closer to the glacier terminus show directional consistency down to the terminus.

Ice velocities in the ablation area of Hailuogou glacier were measured from stake displacements using an optical theodolite in the 1980s and 1990s (Song, 1994; Li and Su, 1996). In earlier work (Li and Su, 1996; Su and others, 1996) it has been suggested that Hailuogou glacier exhibited a

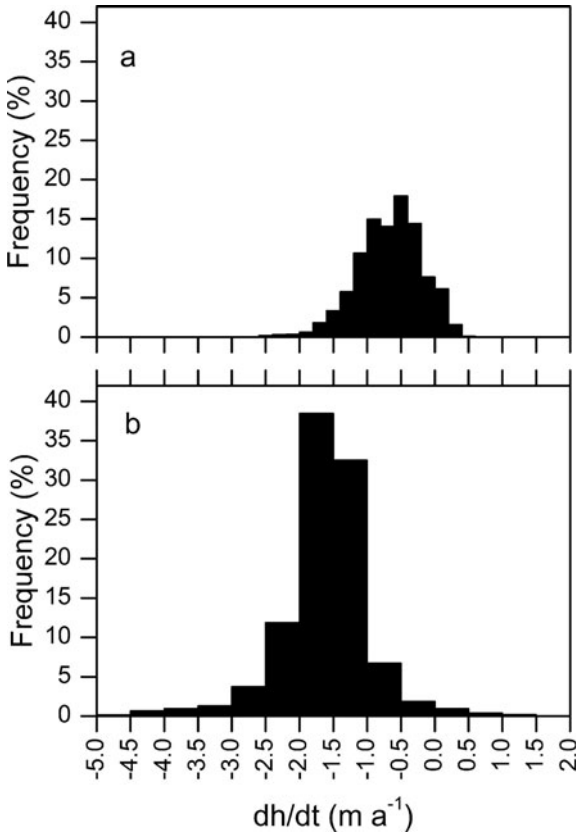

Fig. 9. Histograms of d*h*/d*t* in the ablation area of Hailuogou glacier. (a) 1966–89 using DEM-1989 minus DEM-1966 and (b) 1989–2009 using ASTER DEM minus DEM-1989.

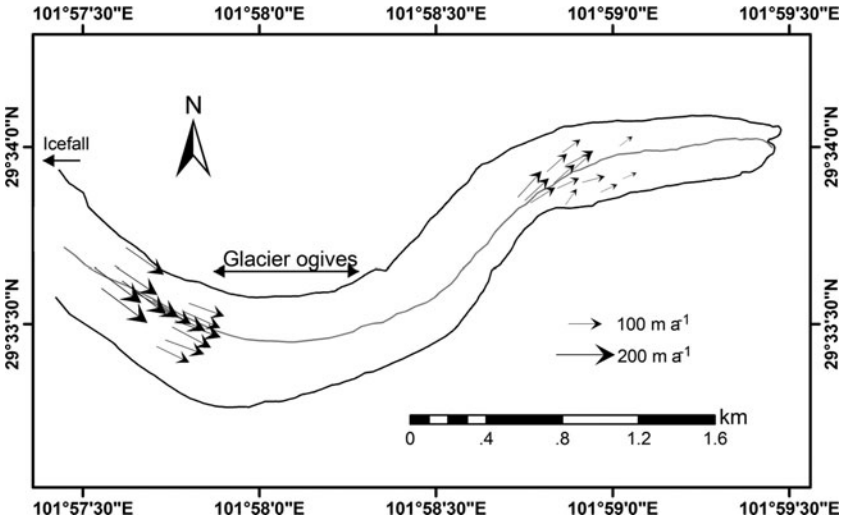

Fig. 10. Vector plot of ice velocity measured in the summer of 2008. Arrow length scales with the measured velocity (m a^{-1}), and arrow direction indicates the direction of the measured velocity. Grey curve is the central flowline.

significant seasonal variation in ice velocity, with the average velocity in summer higher than in winter because of enhanced sliding by rapid migration of surface meltwater to the ice–bedrock interface. Based on field measurements (Song, 1994; Su and others, 1996) the average annual ice velocity had reduced by 30.0 m a^{-1} over the period 1981–98. The variation in summer ice velocity along the central flowline in 1981, 1990 and 2008 is shown in Figure 11a. Ice velocities show minor fluctuations in the lower part of the ablation area but larger fluctuations in the upper part (Fig. 11a). On average, the summer ice velocity in the ablation area has reduced by 31% over the past 28 years.

DISCUSSION

The temporal evolution of a glacier surface can be determined by the vertically integrated continuity equation for incompressible ice by assuming a constant ice density (Van der Veen, 1999):

$$\frac{\partial H}{\partial t} = B - \frac{\partial (UH)}{\partial x}, \qquad (2)$$

where t is time, x is distance along the central flowline, B is the surface mass balance, U is the velocity averaged over the depth, which is often derived from the surface ice velocity (Nye, 1965), and H is the ice thickness, so that UH is the ice flux. It is concluded from Equation (2) that temporal change in surface elevation at each point in the ablation area of Hailuogou glacier varies in response to the mass balance (accumulation and melt) and the ice velocity. Local variations in these factors determine the glacier profile; that is, surface mass balance and ice velocity are the potential contributors to the observed multi-decadal fluctuations in surface elevation. We examine each of these in turn below.

As discussed above, Hailuogou glacier has undergone a significant reduction in ice velocity over the period 1981–2008. Decreases in the average annual and average summer ice velocities are about 24% and 31%, respectively, from those in the 1980s. Previous studies have suggested that the ice flux change is strongly correlated with ice velocity change over the whole area of the glacier (Van der Veen, 1999; Vincent and others, 2009). In other words, the velocities are mainly responsible for the changes in the ice flux. Therefore, simple considerations of force balance on the glacier suggest that a regional thinning will be consistent with slightly lower velocities. This is well correlated with

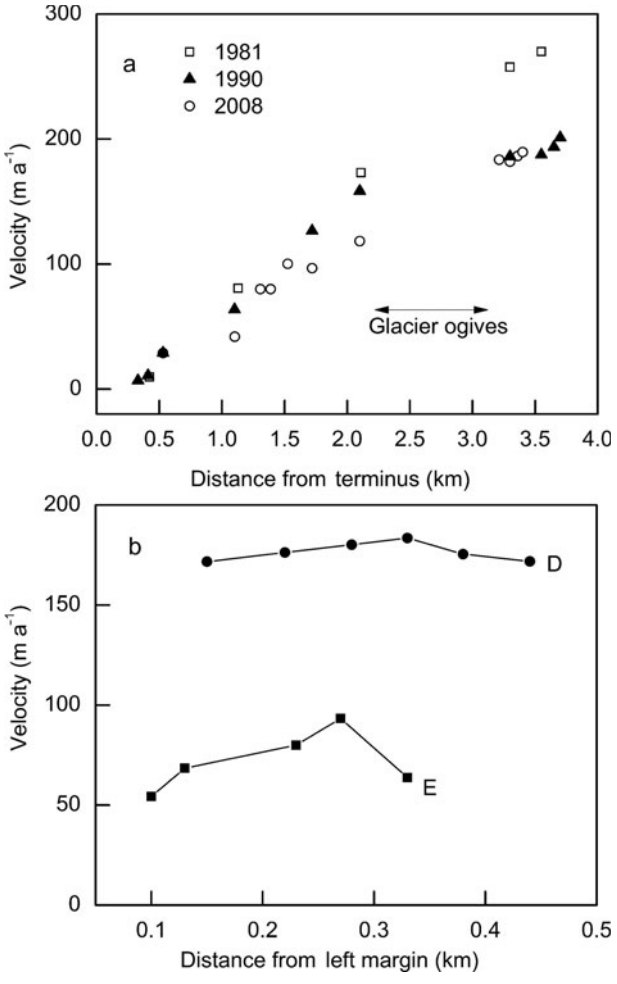

Fig. 11. (a) Ice velocities along the central flowline in the ablation area of Hailuogou glacier in the summer of 1981, 1990 and 2008. (b) Ice velocities at cross-sections D (3475 m a.s.l.) and E (3110 m a.s.l.) indicated in Figure 1 in the summer of 2008.

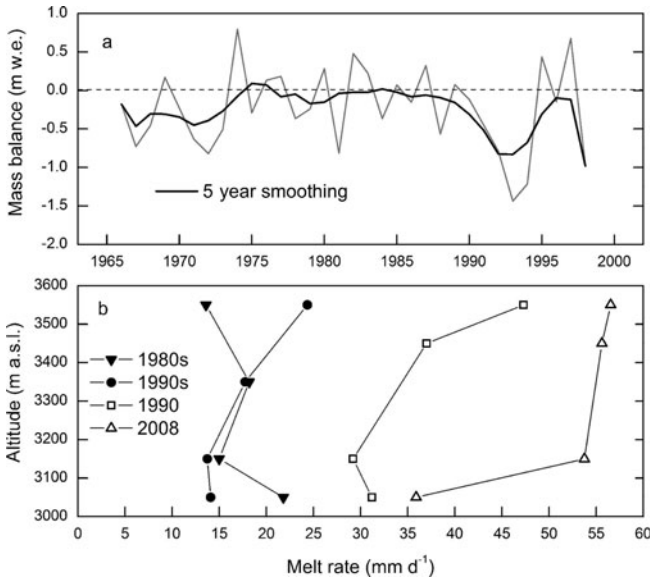

Fig. 12. (a) Mass-balance variation of Hailuogou glacier for the period 1966–98. (b) Glacier melt rate in different periods. Mass-balance data are derived from Aizen and others (1994) and Xie and others (2001); glacier melt data in the 1980s and 1990s are derived from Li and Su (1996) and Su and others (1996).

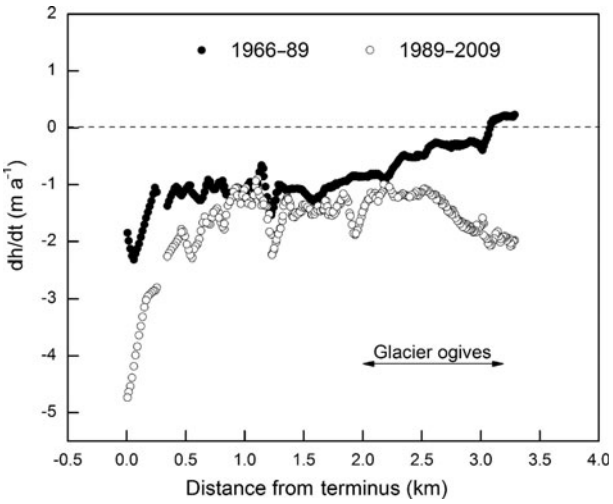

Fig. 13. Surface d*h*/d*t* along the central flowline in the ablation area of Hailuogou glacier.

accelerated retreat of the terminus in past decades, where the ice velocity is the lowest in the entire glacier, tending to 0.0 m a^{-1} (Fig. 11a); on the other hand, the average glacier melt rate indicates a significant increase as shown in Figure 12b.

In past decades, Hailuogou glacier was characterized by negative mass balance (Fig. 12a) (Aizen and others, 1994; Xie and others, 2001). The average annual mass balance was –0.15 m a^{-1} for the period 1966–89 (Aizen and others, 1994) and –0.45 m a^{-1} for the period 1990–98 (Xie and others, 2001). Furthermore, average annual temperature observed at GAEORS indicates a significant increasing trend for the period 1988–2004 (Fig. 5b). The mean temperature over the period 1998–2004 was 0.42°C higher than for the period 1988–97. Over the same period, the temperature at the beginning of the glacier melt season (April) rose by 1.6°C and at the end of the melt season (October) by 0.9°C. This possibly prolongs the melt period and causes a significant decrease in snow accumulation (Fujita, 2008). This can be seen in Figure 12b, which shows the year-on-year increase in glacier melt rate in the ablation area of Hailuogou glacier. Meanwhile, precipitation during July–September decreased by 24% over the period 1998–2004 compared with that for the period 1988–97, especially in July and September. Recently, Helsen and others (2008) have reported a model of the effect of accumulation anomalies on measured surface elevation changes and suggested that elevation change can depend on both current and decadal to multi-decadal average accumulation rate. We note that Hailuogou glacier is a summer-accumulation type glacier (Shi and Liu, 2000). Summer precipitation accounts for more than 80% of the total annual precipitation (Fig. 5a). A reduction in precipitation during July–September possibly has a significant effect on the accumulation on Hailuogou glacier. Thus an increase in glacier melt rate and a decrease in precipitation during July–September are well correlated with accelerated thinning in the ablation area of Hailuogou glacier over the past 20 years.

In the icefall of Hailuogou glacier, the ice flow is dominated by rapid extending flow, whereas it is dominated by compressive flow between the icefall and the zone of glacier ogives (Li and Su, 1996). In this region, the flow is strongly compressive along the central flowline as a result of the change in slope and narrowing of the valley. The walls prevent lateral extension, and the reduction in flow below the icefall must be compensated by extension in the vertical direction. Consequently, this area shows strong emergent flow and shearing, and the glacier between the icefall and the zone of glacier ogives thickens. As shown in Figure 13, the ice in this area indicates a thickening trend for the period 1966–89. During this period the ice velocity in this area was relatively large (Fig. 11a), while the change in glacier mass balance was relatively small over the whole glacier (Aizen and others, 1994). As shown by the observed ablation data in the 1980s (Li and Su, 1996), the glacier melt rates for this area were minimal over the entire ablation area (Fig. 12b). We infer that the surface elevation changes are driven by changes in the compressive flow between the icefall and the zone of glacier ogives during 1966–89. Conversely, for the period 1990–2008 the ice between the icefall and the zone of glacier ogives has shown a significant thinning (Fig. 13). Figure 11a shows a minor change in summer ice velocity during 1990–2008. The magnitude of the (negative) mass balance, however, has increased by a factor of 3 from 0.15 to 0.45 m a^{-1} for the whole glacier (Fig. 12a). Since the 1990s the maximum glacier melt rate in the ablation zone has occurred in this area (Fig. 12b). The average glacier melt rate in this area in the 1990s increased by 79% compared with that in the 1980s. Therefore, the surface elevation changes have been driven mainly by the surface mass-balance change between the icefall and the zone of glacier ogives for the period 1990–2008.

Below the zone of glacier ogives, Figures 7 and 13 reveal dramatic thinning during 1966–2009. Although the negative mass balance of the whole glacier was relatively small for the period 1966–89 (Fig. 12a), the glacier melt rate in the ablation area was a maximum in the 1980s (Fig. 12b). After 1989, the mass loss of the glacier increased (Fig. 12a). Note that the ablation area is covered by thick debris which exerts considerable influence on the surface mass balance and protects the glacier from much more rapid mass loss.

However, the glacier melt rate shows a significant year-to-year increase due to increasing temperatures (Fig. 5b). The glacier melt rate in this area in the summer of 2008 increased by about 48% compared with that in 1990. Due to the different thicknesses of the debris cover distributed in this area, the glacier melt rate was not homogeneous. As a result, there are some large ice cliffs in this area that are usually covered with a thin layer of debris or dust (Fig. 2d). Ablation at such cliffs on the debris-covered glacier plays an important role in the mass balance (Adhikary and others, 2000; Sakai and others, 2002). Previous work suggests that the average melt rate is ten times larger at such ice cliffs than on the less steep debris-covered areas (Adhikary and others, 2000; Sakai and others, 2002). Additionally, changes in ice velocity in this area are relatively small (Fig. 11a). It can be seen that the surface-elevation changes over the past few decades below the zone of glacier ogives are triggered by surface mass-balance changes that are clearly connected to the summer melting.

CONCLUSIONS

We have analyzed a 43 year record (1966–2009) of surface elevation data for the ablation area of Hailuogou glacier and found that its surface elevation has greatly changed in net terms over this period. The average net elevation change rate in the ablation area over the 43 years is $-1.1 \pm 0.4\,\mathrm{m\,a^{-1}}$. Since 1989 the surface lowering has accelerated significantly. Ice velocities in the summer of 2008 show an increasing trend with distance from the glacier terminus. In comparison with the velocities along the central flowline in the 1980s, the average summer ice velocity in 2008 has undergone a significant reduction, especially in the upper part of the ablation area.

In the upper part of the ablation area between the icefall and the zone of glacier ogives, the surface-elevation changes are driven mainly by compressive flow changes for the period 1966–89 and changes in surface mass balance after 1989. Conversely, the surface-elevation changes below the zone of glacier ogives are triggered by surface mass-balance changes that are clearly connected with summer melting. Our results highlight the importance of continuous multi-decadal observations of surface elevation for monsoonal maritime glaciers.

ACKNOWLEDGEMENTS

We thank the Gongga Alpine Ecosystem Observation and Research Station of the Chinese Ecological Research Network for providing temperature and precipitation data. This work was supported by the Innovation Project of the Chinese Academy of Sciences (Kzcx2-yw-301), the National Basic Research Program of the Ministry of Science and Technology of China (2007CB411501), the National Natural Science Foundation of China (40701032) and the National Essential Scientific Program of the Ministry of Science and Technology of China (2006FY110200). This research was also supported by a Grant-in-Aid for Science Research (No. 19253001) from the Ministry of Education, Culture, Sports, Science and Technology of Japan. We thank the reviewers R. Armstrong and R. Gupta, the Scientific Editor T. Scambos and the Chief Editor T.H. Jacka for helpful comments and suggestions.

REFERENCES

Adhikary, S., M. Nakawo, K. Seko and B. Shakya. 2000. Dust influence on the melting process of glacier ice: experimental results from Lirung Glacier, Nepal Himalayas. *IAHS Publ.* 264 (Symposium at Seattle 2000 – *Debris-Covered Glaciers*), 43–52.

Aizen, V.B., S.A. Nikitin and G. Song. 1994. Model of the dynamics of the Hailuogou glacier (southeastern Xizang). *In* Xie, Z. and V.M. Kotlyakov, *eds. Glaciers and environment in the Qinghai-Xizang (Tibet) Plateau (I) – the Gongga Mountain: reports on the Sino-Russian Joint Glaciological Expedition*. Beijing and New York, Science Press, 121–132.

Benn, D.I., S. Wiseman and K.A. Hands. 2001. Growth and drainage of supraglacial lakes on the debris-mantled Ngozumpa Glacier, Khumbu Himal, Nepal. *J. Glaciol.,* **47**(159), 626–638.

Ding, Y., S. Liu, J. Li and D. Shangguan. 2006. The retreat of glaciers in response to recent climate warming in western China. *Ann. Glaciol.,* **43**, 97–105.

Dyurgerov, M. 2002. *Glacier mass balance and regime: data of measurements and analysis*. Boulder, CO, University of Colorado. Institute of Arctic and Alpine Research. (INSTAAR Occasional Paper 55.)

Fujisada, H., G.B. Bailey, G.G. Kelly, S. Hara and M.J. Abrams. 2005. ASTER DEM performance. *IEEE Trans. Geosci. Remote Sens.,* **43**(12), 2707–2714.

Fujita, K. 2008. Effect of precipitation seasonality on climatic sensitivity of glacier mass balance. *Earth Planet. Sci. Lett.,* **276**(1–2), 14–19.

Fujita, K., R. Suzuki, T. Nuimura and A. Sakai. 2008. Performance of ASTER and SRTM DEMs, and their potential for assessing glacial lakes in the Lunana region, Bhutan Himalaya. *J. Glaciol.,* **54**(185), 220–228.

Guo, C.-X., M. Bo, Z. Ji and L. Mao. 2002. The transfer model between the Xi'an 80 and WGS-84 coordinate systems. *Northeast Surv. Map.,* **25**(4), 34–36. [In Chinese with English summary.]

Helsen, M.M. *and 7 others*. 2008. Elevation changes in Antarctica mainly determined by accumulation variability. *Science,* **320**(5883), 1626–1629.

Kaser, G., J.G. Cogley, M.B. Dyurgerov, M.F. Meier and A. Ohmura. 2006. Mass balance of glaciers and ice caps: consensus estimates for 1961–2004. *Geophys. Res. Lett.,* **33**(19), L19501. (10.1029/2006GL027511.)

Kick, W. 1962. Variations of some central Asiatic glaciers. *IASH Publ.* 58 (Symposium at Obergurgl 1962 – *Variations of the Regime of Existing Glaciers*), 223–229.

Li, J. and Z. Su, *eds*. 1996. *Glaciers in the Hengduanshan.* Beijing, Science Press. [In Chinese with English summary.]

Liu, S., W. Sun, Y. Shen and G. Li. 2003. Glacier changes since the Little Ice Age maximum in the western Qilian Shan, northwest China, and consequences of glacier runoff for water supply. *J. Glaciol.,* **49**(164), 117–124.

Liu, S. *and 7 others*. 2006. Glacier retreat as a result of climate warming and increased precipitation in the Tarim river basin, northwest China. *Ann. Glaciol.,* **43**, 91–96.

Lu, A., T. Yao, S. Liu, L. Ding and G. Li. 2002. Glacier change in the Geladandong area of the Tibetan Plateau monitored by remote sensing. *J. Glaciol. Geocryol.,* **24**(5), 559–562. [In Chinese with English summary.]

Mair, D., P. Nienow, I. Willis and M. Sharp. 2001. Spatial patterns of glacier motion during a high-velocity event: Haut Glacier d'Arolla, Switzerland. *J. Glaciol.,* **47**(156), 9–20.

Nakawo, M., H. Yabuki and A. Sakai. 1999. Characteristics of Khumbu Glacier, Nepal Himalaya: recent changes in the debris-covered area. *Ann. Glaciol.,* **28**, 118–122.

Nye, J.F. 1965. The flow of a glacier in a channel of rectangular, elliptic or parabolic cross-section. *J. Glaciol.,* **5**(41), 661–690.

Oerlemans, J. and J.P.F. Fortuin. 1992. Sensitivity of glaciers and small ice caps to greenhouse warming. *Science,* **258**(5079), 115–117.

Paterson, W.S.B. 1994. *The physics of glaciers. Third edition.* Oxford, etc., Elsevier.

Rignot, E., A. Rivera and G. Casassa. 2003. Contribution of the Patagonian icefields of South America to sea level rise. *Science,* **302**(5644), 434–437.

Sakai, A., M. Nakawo and K. Fujita. 2002. Distribution characteristics and energy balance of ice cliffs on debris-covered glaciers, Nepal Himalaya. *Arct. Antarct. Alp. Res.,* **34**(1), 12–19.

Shangguan, D. *and 9 others*. 2006. Monitoring the glacier changes in the Muztag Ata and Konggur mountains, east Pamirs, based on Chinese Glacier Inventory and recent satellite imagery. *Ann. Glaciol.,* **43**, 79–85.

Shi, Y. and S. Liu. 2000. Estimation on the response of glaciers in China to the global warming in the 21st century. *Chinese Sci. Bull.,* **45**(7), 668–672. [In Chinese.]

Shi, Y., C. Liu, Z. Wang, S. Liu and B. Ye, *eds*. 2005. *A concise China glacier inventory.* Shanghai, Shanghai Science Popularization Press. [In Chinese.]

Solomon, S. *and 7 others, eds*. 2007. *Climate change 2007: the physical science basis. Contribution of Working Group I to the Fourth Assessment Report of the Intergovernmental Panel on Climate Change.* Cambridge, etc., Cambridge University Press.

Song, G. 1994. Movement features of Hailuogou glacier in the Gongga Mountain. *In* Xie, Z. and V.M. Kotlyakov, *eds. Glaciers and environment in the Qinghai–Xizang (Tibet) Plateau (I) – the Gongga Mountain: reports on the Sino-Russian Joint Glaciological Expedition.* Beijing and New York, Science Press, 110–120.

State Bureau of Surveying and Mapping of China (SBSMC). 2000. *Quality requirement for digital products of surveying and mapping – Part 1: quality requirement for digital line topographic map, digital elevation model.* Beijing, Standards Press of China. (Standard No. GB/T 17941–2000.) [In Chinese.]

Su, Z., S. Liu, N. Wang and A. Shi. 1992. Recent fluctuations of glaciers in the Gongga mountains. *Ann. Glaciol.,* **16**, 163–167.

Su, Z., G. Song and Z. Cao. 1996. Maritime characteristics of Hailuogou glacier in the Gongga Mountains. *J. Glaciol. Geocryol.,* **18**, Special Issue, 51–59. [In Chinese with English summary.]

Van der Veen, C.J. 1999. *Fundamentals of glacier dynamics.* Rotterdam, A.A. Balkema.

Vincent, C., A. Soruco, D. Six and E. Le Meur. 2009. Glacier thickening and decay analysis from 50 years of glaciological observations performed on Glacier d'Argentière, Mont Blanc area, France. *Ann. Glaciol.,* **50**(50), 73–79.

Wang, J.X., J. Wang and C.P. Lu. 2003. Problem of coordinate transformation between WGS-84 and BEIJING 54. *J. Geod. Geodyn.,* **23**(3), 70–73. [In Chinese.]

Willis, I., D. Mair, B. Hubbard, P. Nienow, U.H. Fischer and A. Hubbard. 2003. Seasonal variations in ice deformation and basal motion across the tongue of Haut Glacier d'Arolla, Switzerland. *Ann. Glaciol.,* **36**, 157–167.

Xie, Z., Z. Su, Y. Shen and Q. Feng. 2001. Mass balance and water exchange of Hailuoguo glacier in Mount Gongga and their influence on glacial melt runoff. *J. Glaciol. Geocryol.,* **23**(1), 7–15. [In Chinese with English summary.]

Yao, T.D., Y.Q. Wang, S.Y. Liu, J.C. Pu, Y.P. Shen and A.X. Lu. 2004. Recent glacial retreat in High Asia in China and its impact on water resource in Northwest China. *Sci. China D,* **47**(12), 1065–1075.

Ye, Q., T. Yao, S. Kang, F. Chen and J. Wang. 2006. Glacier variations in the Naimona'nyi region, western Himalaya, in the last three decades. *Ann. Glaciol.,* **43**, 385–389.

Zhang, Y., S. Liu, J. Xu and D. Shangguan. 2008. Glacier change and glacier runoff variation in the Tuotuo River basin, the source region of Yangtze River in western China. *Environ. Geol.,* **56**(1), 59–68.

MS received 27 March 2009 and accepted in revised form 30 November 2009